BIOCHAR MODIFICATION, THERMAL STABILITY AND TOXICITY OF PRODUCTS MODIFICATION

Petra ROUPCOVÁ[1], Romana FRIEDRICHOVÁ[2], Karel KLOUDA[3], Markéta WEISHEITELOVÁ[4], Michaela PERĎOCHOVÁ[5]

Research article

Abstract: Biochar is a product obtained from processing of waste biomass. The main application of biochar is in soil and environment remediation. Some new applications of this carbonaceous material take advantage of its adsorption capacity use it as a heterogeneous catalyst for energy storage and conversion etc. This contribution describes thermal stability of the original biochar. It discusses biochar modified by chemical and physical methods including a new compound of biochar-graphene oxide. The purpose of the modifications is to increase its active surface to introduce active functional groups into the carbon structure of biochar in relation to fire safety and toxicity of those products.

Keywords: Biochar, soil remediation, thermal stability, fire safety, ecotoxicity.

Introduction

The raw material for preparation of biochar is biomass from diverse sources, e.g. cow and pig manure, straw, grass, corn, wood waste, sludge from wastewater treatment plants or a solid portion of digestate after biomass fermentation process.

The basic technology for preparation of biochar is slow pyrolysis at 300-600 °C with limited or no access of air. Another variant is hydrothermal (wet) pyrolysis performed at lower temperatures, ca. 200 °C.

Pyrolysis or hydrothermal pyrolysis produces a porous carbonaceous product with a more compact hydrophobic core with mostly aromatic structure, covered with a hydrophilic shell with some chemical activity associated with oxygen-containing functional groups.

Biochar can be characterized with physical, chemical and hydraulic properties:

- physical - size and distribution of particles, density, surface area, volume of pores (porosity);
- chemical - red-ox potential, pH, content of O, H, C and their ratio, zeta potential, content of heavy metals, PAU content;
- hydraulic - content of water leachate, humidity, hydraulic conductivity, absorbability.

Use of biochar

Biochar is a material with a number of potential applications but its properties can be influenced by many factors. They include the type of processed biomass, selection of technological procedure (pyrolysis, thermal pyrolysis), temperature, temperature gradient, reaction time etc. Its properties can be changed by the so-called modification, e.g. increase of volume of pores, increase of specific surface, change of representation of functional groups on the surface or by introduction of nanoparticles of metals or metal oxides into the biochar structure. The modification of biomass can be performed before pyrolysis, by addition of a catalyst (alkali hydroxides) or metal salts that are

[1] VŠB - Technical University of Ostrava, Faculty of Safety Engineering, Ostrava, Czech Republic, petra.roupcova@vsb.cz

[2] Ministry of Interior - General Directorate of the Fire and Rescue Service of the Czech Republic, Prague, Czech Republic, romana.friedrichova@grh.izscr.cz

[3] VŠB - Technical University of Ostrava, Faculty of Safety Engineering, Ostrava, Czech Republic, karel.klouda@vsb.cz

[4] State Office for Nuclear, Chemical and Biological Protection, Kamenná, Czech Republic, weisheitelova@sujbcho.cz

[5] VŠB - Technical University of Ostrava, Faculty of Safety Engineering, Ostrava, Czech Republic, michaela.perdochova@vsb.cz

reduced during pyrolysis to metal or metal oxide nanoparticles. Other methods include chemical and physical treatment of biochar after the pyrolysis. In most cases it involves chemical modification seeking to change functional groups on the surface by oxidation, sulfonation, amidation or reaction of monomers (oligomers) to form composite materials. Physical modifications include sonication or turbo milling (one method for preparation of magnetic biochar).

An overview of examples of published procedures for biochar modification before and after pyrolysis is provided in Tab. 1.

Tab. 1 Overview of published procedures for biochar modification

Agent used for modification	Modification by pyrolysis		Note to the content of the publication	LO
	Before	After		
CH_3OH		+	Improvement of adsorption capacity to tetracycline	(Jing et al., 2014)
H_2O_2		+	Utilization of the role of - OH radicals	(G. Fang et al., 2014)
$FeCl_2$, $FeSO_4$, $Ni(NO_3)_2$		+	Preparation of magnetic biochar	(Safarik et al., 2012)
GRAPHITE+ Py-SO_3	+		Sorption material for PAU sorption	(Zhang et al., 2012)
$KMnO_4$, HNO_3		+	Testing of changes of adsorption capacity	(Li et al., 2014)
KOH, HNO_3, H_2SO_4, H_2O_2, $KMnO_4$		+	Changes of surface area, structure and volume of pores	(Yakout et al., 2015)
Sea weeds	?	?	Electrochemical process	(Jung et al., 2015)
$MgCl_2$	+		Capture of phosphate ions	(C. Fang et al., 2014)
Active coal	+		For capture of PAU	(Oleszczuk et al., 2012)
H_2O_2, O_3, $KMnO_4$, HNO_3		+	Introduction of oxo groups on the surface	(Liu et al., 2015)
H_2SO_4		+	Introduction of -SO_3 group with surface catalysts	(Liu et al., 2015)
Nanoparticles of metals, $Fe(NO_3)_3$, $Ni(NO_3)_2$	+		Introduction of metal nanoparticles into the structure	(Liu et al., 2015)
Monomers, oligomers, polymers		+	Preparation of polymer composite materials	(Das et al., 2015)
KOH, NaOH	+		Preparation of a catalyst of alkaline character	(Abdul Hamid et al., 2014)
HNO_3, H_2SO_4		+	Improvement of adsorption capacity to Cd and Al ions	(Qian et al., 2015)
Metal salts (Fe, Pd, Pt, Ni)	+		Preparation of a catalyst biochar - metal	(Shen, 2015)
KOH, NaOH	+		Increase of biochar surface	(Gu and Wang, 2013)
Fe^{2+}, Fe^{3+}, SO_4^{2-}	+	+	Preparation of magnetic biochar	(Tan et al., 2016)
Clays, kaolin, montmorillonite	+		New material - testing of adsorption kinetics (methylene blue)	(Yao et al., 2014)
H_2SO_4, solution KOH		+	Improvement of adsorption capacity to tetracycline	(P. Liu et al., 2012)
HNO_3 50 %		+	Formation of carbonaceous nanoparticles	(Manav et al., 2016)
CNT (0.01-1%)	+		Improvement of sorption capacity	(Inyang et al., 2014)
Lignite	+		Joint processing - hydrothermal	(Z. Liu et al., 2012)
$MnCl_2 . 4H_2O$	+		Modification of biochar with MnO_x Improvement of sorption capacity to As and Pb	(Wang et al., 2015)
$KMnO_4$ + HCl		+	Preparation of composite Birnessite - Biochar	(Wang et al., 2015)
HNO_3 + H_2SO_4 (1:1) + $Na_2S_2O_4$		+	Amidation of biochar (reduction of NO_2 groups to - NH_2), increase of sorption capacity to Cu^{2+}	(Yang and Jiang, 2014)
Chitosan		+	Sorption of heavy metals and biological activity	(Zhou et al., 2013)
Fe_3O_4		+	Preparation of sorbents in a ball mill - sorption capacity to antibiotics	(Shan et al., 2016)

Legend: LO - Reference

The Biochar Journal (Schmidt and Wilson, 2014) magazine published 55 examples of biochar utilization with potential commercialization. In addition to specific utilization opportunities (Yao and Wu, 2015; Zhang et al., 2014), such as heterogeneous catalyst with a broad field of application, material for energy storage and conversion as a supercapacitator or Li-battery, the main application of biochar is in soil engineering and as an adsorbent for various inorganic and organic pollutants, both in water and soil environment - see below. In respect to agriculture (soil), biochar is recognized to have the following benefits (Krishnakumar et al., 2014):

- increases water capacity of soil;
- increases production of biomass;
- increases pH of soil;
- reduces toxicity of aluminum;
- reduces tensile strength of soil;
- changes (supports) microbial activity;
- reduces emissions of CO_2, N_2O, CH_4 from soil, adsorbs organic and inorganic compounds.

The last reference is also connected with the important capacity of biochar to adsorb both inorganic substances (heavy metal ions) and organic contaminants in water environment and in soils, while it acts as a sorbent and prevents or limits undesired substances in plants. Physicochemical properties of biochar influence the adsorption kinetics. They are mainly the surface area, porosity and functional groups on the surface. Those properties are affected by the type of the initial biomass, temperature and duration of pyrolysis (hydropyrolysis), level of carbonization, pH of the solution in which the adsorption occurs, coexistence of cations, dosing (concentration) of biochar as an adsorbent, temperature (Note: adsorption is an endothermic process) etc. There is a number of mechanisms between the biochar surface and the adsorbed substance, such as electrostatic attraction, chemical bonds, intercalation, hydrogen bonds, π-π interaction, fixing in pores, hydrophobic interaction etc. (Tan et al., 2015). Prevailing mechanisms have been demonstrated for adsorption of certain specific substances. For example, for trichloroethylene it was filling of pores (Ahmad et al., 2013) and for aromatic explosives (TNT) it was π-π interaction (Oh and Seo, 2014). There are also examples of adsorption of metal ions of chromium (Karim et al., 2015), lead (Lu et al., 2012), uranium (Kumar et al., 2011), zinc and copper (Chen et al., 2011) and a whole range of groups of organic substances which may have a negative impact on the environment. They are pesticides (Taha et al., 2014; Trigo et al., 2014; Sun et al., 2011), worldwide-used pharmaceutical products, such as isobrufen (Essandoh et al., 2015), tetracycline (Liao et al., 2013), acetaminophenon (Im et al., 2014), aspirin (Essandoh et al., 2015) toxic industrial substances (Chen and Chen, 2009; Wang et al., 2013), explosives (Oh and Seo, 2014; Oh and Seo, 2015) etc.

Potential negative factors of biochar

Biochar toxicity

Depending on the type of raw material (biomass) and the method of its pyrolysis, biochar can have a higher content of heavy metals, polyaromatic carbohydrates and various metabolites. During pyrolysis biochar can be contaminated with condensed pyrolytic vapors (Tang et al., 2016) - it is a process of the so-called release of mobile organic compounds. Electron paramagnetic resonance has shown that biochar also contains persistent free radicals that may cause inhibition of plant growth.

As the main application of biochar is in soil it is subject to environmental monitoring, i.e. tests of phytotoxicity - germination, root elongation, plant growth, tests of escape behavior annelid worms, effects on soil microflora, behavior of biochar in soil organic matter etc. (Lehmann et al., 2011)

Exposure to dust and fire hazards

Fire hazards are posed by the technology used for biomass processing and also by its products. The products are combustible and explosive gases (CH_4, CO, H_2, C_nH_{2n+2}), bio-oils (a liquid component) and biochar (a solid component). Biochar consists mainly of carbon-based powdery components which, depending on the surface area, size of particles, volume of pores and humidity, may form an explosive mixture with air. Safety data sheets of randomly selected three commercial biochar producers (Aemerge, Confluence, U. S. Department of Labor) indicate the minimum explosive concentration of biochar 0.14 g/L. One work published in 2012 (Dzonzi-undi et al., 2014) dealt with determination of self-ignition parameters of biochar during storage in relation to the surrounding temperature and the biochar volume. At the surrounding temperature of 25 °C it is 5.3 m^3 biochar on a heap while at 40 °C it is only 0.75 m^3. The exposure limit in safety data sheets is 15 mg/m^3 and for respirable particles it is 5 mg/m^3.

Introduction of rules for biochar standardization

The European section of the International Biochar Initiative grants European Biochar Certificates to commercial producers (EBC www.Europen-biochar.org/en/ebc-ibi). To obtain the certificate it is necessary to submit and to document results of analyses of density, electric conductivity, pH, content of C, H, O, N, ash and heavy metals, PAU and TGA diagram.

Data about thermal stability of biochar and its modifications published in this paper contribute to comprehensiveness of the doctoral research at FBI VŠB-TU in the fields of ecotoxicity and sorption capacity of biochar and its modifications.

Material and methods

Biochar: prepared by pyrolysis of biomass consisting of 80 % of corn silage and 20 % cellulose fibers, 470 °C, 17 min. The pyrolysis was performed by Biouhel s.r.o Zlín. Biochar made of condensate (FB-1) and flue dust (FB-2).

Instrumentation

Measurement of FT-IR spectrums: Spectrometer Brucker Alpha/FT-IR, software OPUS 6.5., measuring range 375-4000 cm^{-1}.

TG-DTA and TG-DSC analysis: STA i 1500 (Instrument Specialists Incorporated - THASS), degradation medium: air, air flow rate 20 ml/min, temperature regime 25-600 °C, sample heating rate 10 °C/min, sample weights FB-1 9.70 mg, FB-2 9.31 mg, FB-3 9.41 mg, FB-4 10.50 mg, FB-5 10.13 mg, FB-6 2.62 mg, FB-7 9.64 mg, FB-8 1.76 mg, FB-9 1.89 mg, FB-10 4.06 mg.

Sonication: NOTUS - Po wersonic s.r.o., Slovakia, Type PS 04000 A, 450 W.

An overview of the chemical reactions and the physical treatments with identification of products is shown in Fig. 1.

We have used the Hummers method for joint oxidation of biochar and graphite in various weight ratios of graphite / biochar from 0 to 2. The total weight of the sample (biochar + graphite) was 2.25 g and the oxidizing mixture consisted of 52 ml of concentrated sulfuric acid, 3.0 g $NaNO_3$ and after cooling of the mixture 10 °C 7.0 g of $KMnO_4$ was gradually added. After that the reaction mixture was gradually heated to 55 °C and intensely stirred for 2-3 hours. Then it was left to stand at the laboratory temperature for 3-4 days. Subsequently the sample was diluted with distilled water, decanted and H_2O_2 and HCl were added. Centrifugation with decantation was repeated until pH was neutral and until a negative reaction to sulfate ions. Depending on its physical constitution the centrifuged product was either filtered or processed into a foil. In the case of FB-10 a part of the product was processed by lyophilization.

Results and discussion

We have divided this chapter into a part that compares structures and thermal stability of the initial biochars and a part that compares the foils prepared from the biochars by Hummers oxidation method while using the same initial ratio biochar - graphite (1:2). The third part contains a discussion of the effects of graphite share used in the Hummers oxidation method to get the final product (powder, foil etc.) The last part contains results of some simple chemical and physical modifications.

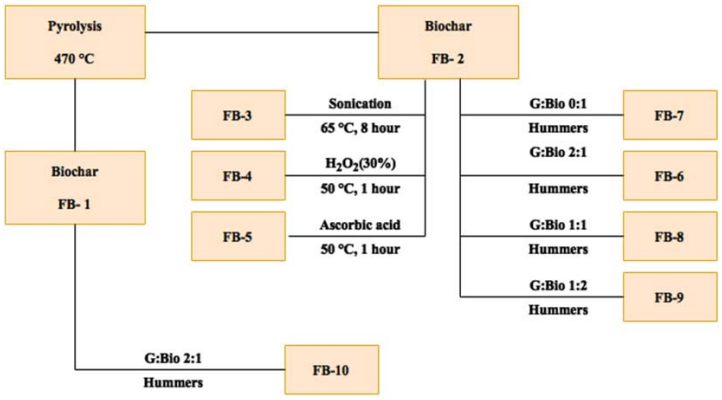

Fig. 1 Biochar diagram

DOI 10.1515/tvsbses-2017-0012

Comparison of the initial biochars

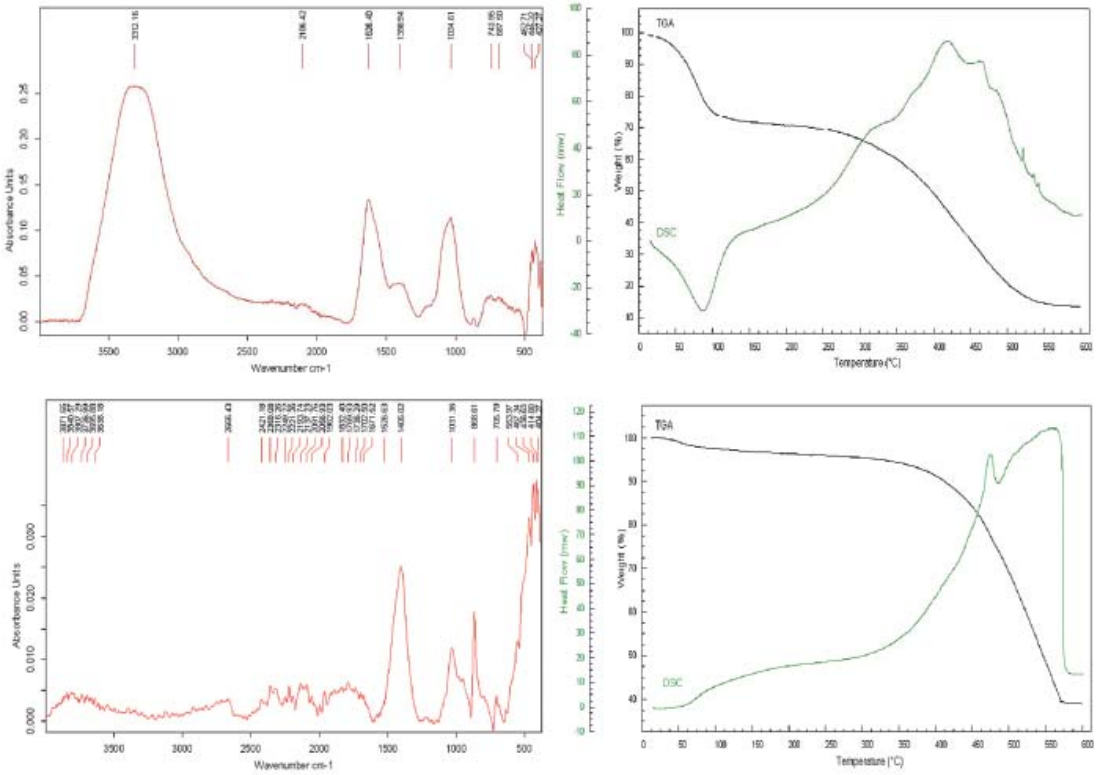

Fig. 2 FT-IR and thermal analyses of initial biochars FB-1and FB-2 [a) IR- spectrum FB-1; b) TGA and DSC curves FB-1; c) IR- spectrum FB-2; d) TGA and DSC curves FB-2]

Comparison of foils prepared by joint oxidation of biochars (FB-1 and FB-2) and graphite (1 : 2)

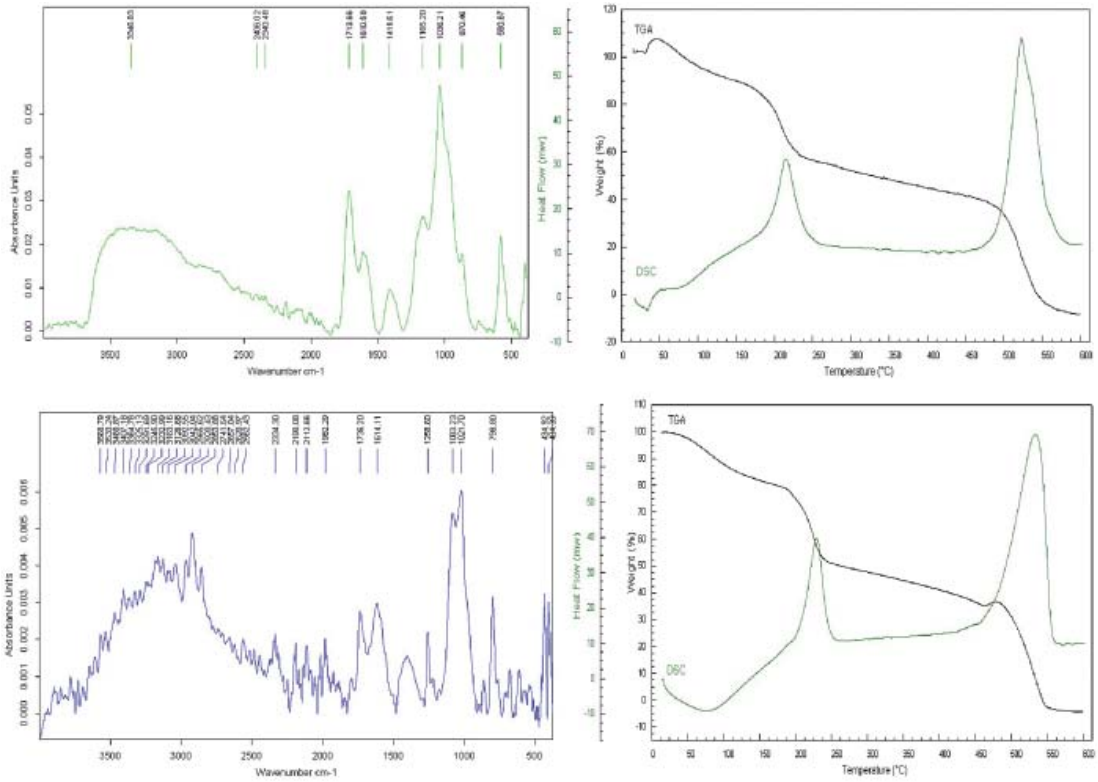

Fig. 3 FT-IR and thermal analysis of products of joint oxidation biochars FB-1 and FB-2 with graphite in the same ratio 1 : 2 [a) IR spectrum FB-6; b) TGA and DSC curves FB-6; c) IR spectrum FB-10; d) TGA and DSC curves FB-10]

Effects of graphite quantity on the character of the product of joint oxidation of graphite and FB-2 using the Hummers method

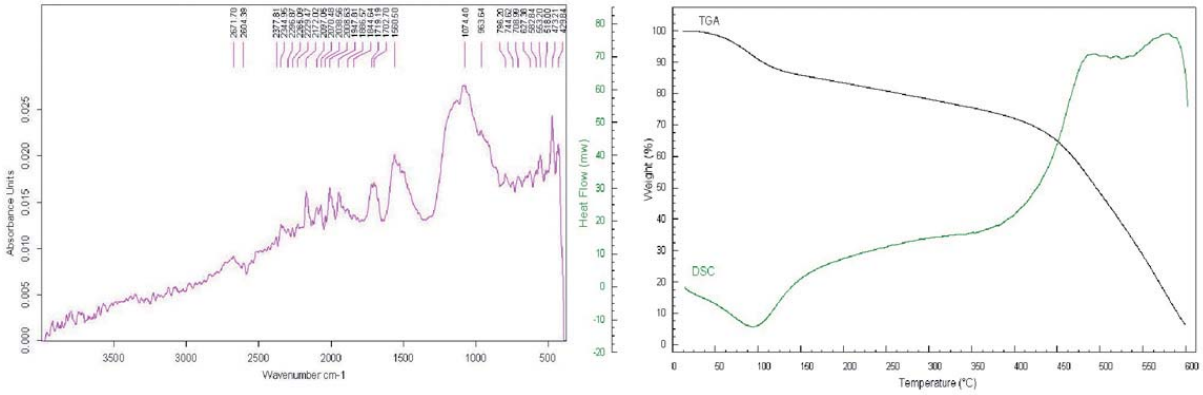

Fig. 4 FT-IR and thermal analysis of the product of oxidation of biochar FB-2 using the Hummers method without graphite: a) IR spectrum FB-7; b) TGA and DSC curves FB-7

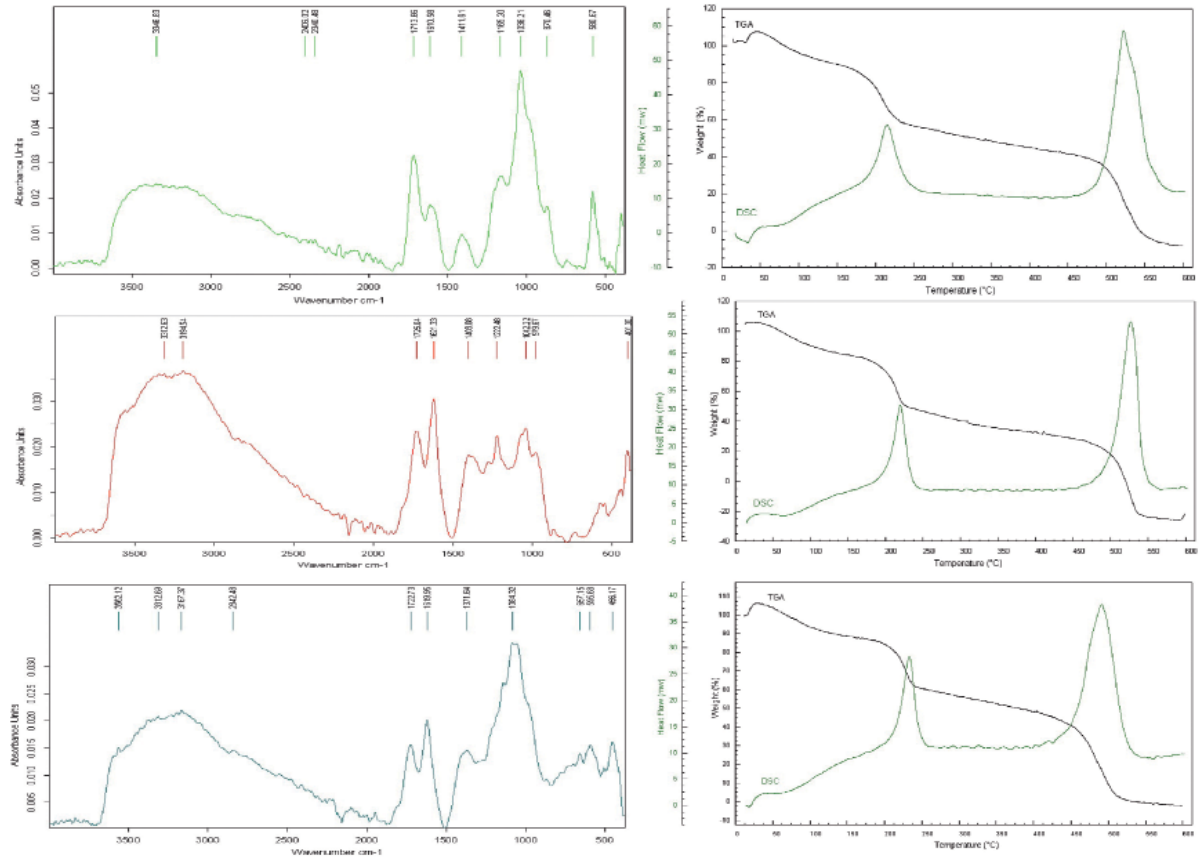

Fig. 5 FT - IR and thermal analysis of products of joint of oxidation of biochar FB - 2 and graphite in different weight ratios [a)IR - spectrum FB-6; b) TGA and DSC curves FB-6; c) IR - spectrum FB-8; d) TGA and DSC curves FB-8; e) IR- spectrum FB-9; f) TGA and DSC curves FB-9]

DOI 10.1515/tvsbses-2017-0012

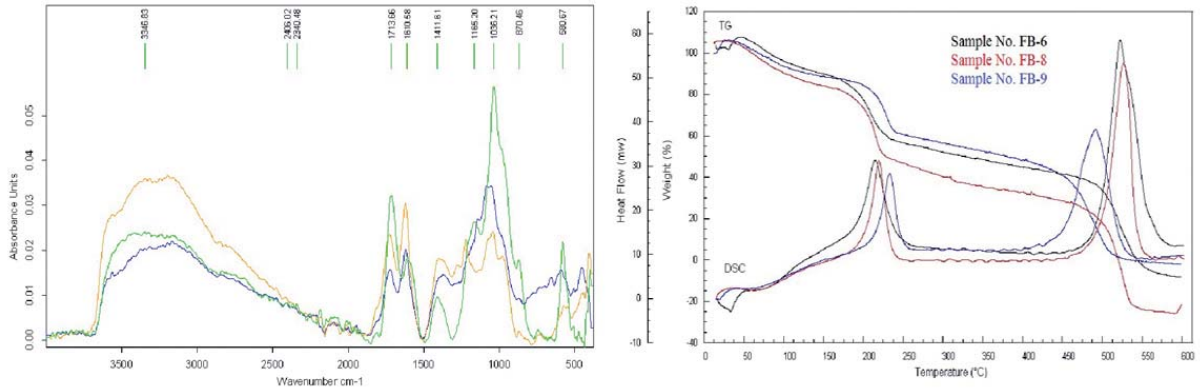

Fig. 6 Summary comparison of IR spectrums and TGA and DSC curves for products of joint oxidation of biochar (FB-2) with graphite in different weight ratios (FB-6, FB-8, FB-9)

Simple chemical modification (with hydrogen peroxide, ascorbic acid) and sonication of biochar FB-2

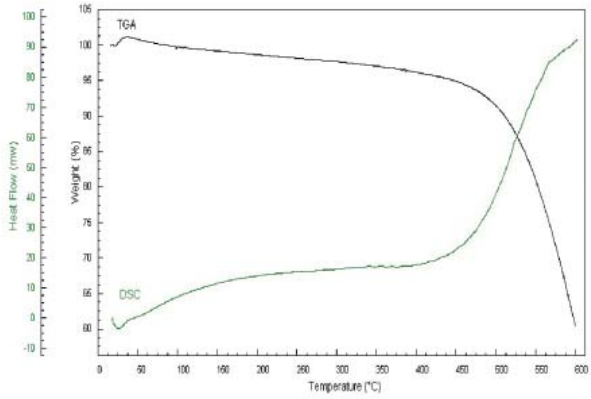

Fig. 7 Thermal analysis (TGA and DSC) of the product FB-3 after physical treatment (sonication) of biochar FB-2

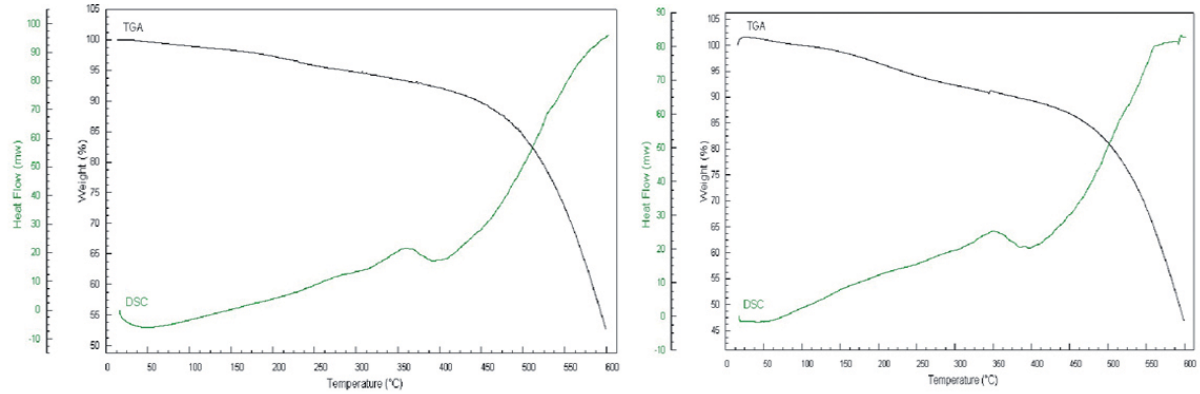

Fig. 8 Thermal analysis (TGA and DSC) of the product after chemical treatment of biochar FB-2: a) TGA and DSC curves of the product FB-4 (oxidation); b) TGA and DSC curves of the product FB-5 (ascorbic acid)

Interpretation of the measured TGA and DSC curves - thermal stability of the prepared products

The TGA curve of the samples No. 1 through 10 can be divided into several sections with different slopes, i.e. rates of weight loss. This division with the respective temperature intervals and weight losses contains parameters of detected thermal processes on the DSC curve. The energy change of the thermal process (ΔH) was determined as an area under a peak corresponding to the respective thermal process, i.e. as the area outlined by a DSC curve and a line between points indicating the beginning and end of the thermal process. The area under the peak is directly proportionate to the heat released or consumed in the reaction and the height of peak (Hf1) is directly proportionate to the reaction rate.

On a DSC curve of the sample FB-1 one peak was detected representing an endothermic process and one peak corresponding to a combination of exothermic processes. The endothermic process occurs in the temperature interval 13.1-129.3 °C with the minimum at 84.0 °C and with the peak area under the DSC curve 1258.6 kJ/kg and it is accompanied by a big weight loss by 25.4 wt. %. The exothermic process in the temperature interval 242.5-599.7 °C with the peak area under the DSC curve 6655.5 kJ/kg and with maximum at 416.1 °C is made up of several processes that cannot be differentiated. Also in this case there is a significant weight loss of the sample.

On a DSC curve of the sample FB-2 one peak was detected corresponding to an endothermic process and one peak corresponding to more exothermic processes. An indistinct endothermic process, associated probably with a delay in heat transfer to the sample, occurs in the temperature interval 13.1-81.5 °C with the minimum at 23.0 °C and the peak area under the DSC curve is 124.3 kJ/kg. The exothermic process is probably made up of several, mutually overlapping thermal processes in the temperature interval 315.2-579.1 °C with the peak area under the DSC curve -7813.6 kJ/kg and with the maximum 554.1 °C. This thermal process is accompanied by a significant weight loss by 50.9 wt. %.

On a DSC curve of the sample FB-3 one peak was detected corresponding to an endothermic process and an indication of an exothermic process. In the temperature interval 16.2-42.0 °C there is an endothermic process with the peak area under the DSC curve 72.9 kJ/kg and it is probably associated with heat transfer to the sample. This process has the minimum at 24.0 °C. In the temperature interval 428.4-599.6 °C there is an indication of an unfinished exothermic process accompanied by a significant weight loss of the sample by 33.6 wt. % in the measured interval of temperatures.

On a DSC curve of the sample FB-4 one peak was detected corresponding to an endothermic process and two peaks corresponding to exothermic processes. The indistinct endothermic process is probably associated with a delay in heat transfer to the sample in the temperature interval 13.8-111.5 °C with the maximum at 44.4 °C and the peak area under the DSC curve is 247.6 kJ/kg. The first exothermic process is also indistinct and it occurs in the temperature interval 307.7-394.0 °C with the peak area under the DSC curve -119.5 kJ/kg with the maximum at 356.6 °C. This process is continually followed by an unfinished exothermic process in the temperature interval 394.0-599.7 °C and it is accompanied by a significant weight loss of the sample by 35.5 wt. % in the interval of measured temperatures.

On a DSC curve of the sample FB-5 one peak was detected corresponding to an endothermic process and two peaks corresponding to exothermic processes. The indistinct endothermic process occurs in the temperature interval 15.8-77.5 °C with the maximum at 37.0 °C and with the peak area under the DSC curve 80.9 kJ/kg. The first exothermic process, also indistinct, occurs in the temperature interval 300.3-382.6 °C with the peak area under the DSC curve 118.3 kJ/kg and with the maximum at 346.8 °C. This process is continually followed by an unfinished exothermic process in the temperature interval 397.1-599.8 °C and it is accompanied by a significant weight loss of the sample by 36.8 wt. % in the interval of measured temperatures.

The shapes of curves of the samples No. FB-3, FB-4 and FB-5 are very similar but in the case of the sample FB-3 the indistinct exothermic process is missing in the temperature interval ca. 300-390 °C. Samples FB-3 and FB-5 demonstrated a slight increase of weight at temperatures up to ca. 35 °C.

On a DSC curve of the sample FB-7 one peak was detected corresponding to an endothermic process and one distinct exothermic process. The endothermic process occurs in the temperature interval 12.2-148.9 °C with the maximum at 90.7 °C and the peak area under the DSC curve is 712.8 kJ/kg. The distinct exothermic process is probably composed of two processes as it is obvious that it was not completed within the interval of measured temperatures. It occurs in the temperature interval 375.5-599.9 °C with the maximum at 576.2 °C and the peak area under the DSC curve

is - 2418.3 kJ/kg. This process is accompanied by a significant weight loss of the sample by ca. 62 wt. %.

A visual inspection of the sample residues after the thermal degradation has shown that residues of the samples FB-1, FB-2 and FB-7 were in the form of brown and white fly ash. The look of the samples FB-3, FB-4 and FB-5 remained practically unchanged, only on the sample surface there was a thin layer of light-colored fly ash.

On a DSC curve of the sample FB-6 one peak was detected corresponding to an endothermic process and two peaks corresponding to exothermic processes. The endothermic process is indistinct and it occurs in the temperature interval 15.1-47.9 °C with the peak area under the DSC curve 286.2 kJ/kg and with the minimum at 30.7 °C. The first exothermic process occurs in the temperature interval 177.3-263.0 °C with the peak area under the DSC curve -1005.6 kJ/kg and with the maximum at 212.2 °C. The second exothermic process occurs in the temperature interval 458.3-591.8 °C with the peak area under the DSC curve -4001,8 kJ/kg and with the maximum at 519.9 °C. Both the exothermic processes are accompanied by significant weight losses.

On a DSC curve of the sample FB-8 two peaks were detected corresponding to exothermic processes. The first exothermic process occurs in the temperature interval 179.7-246.2 °C with the maximum at 217.1 °C and with the peak area under the DSC curve 1319,2 kJ/kg. The second exothermic process occurs in the temperature interval 453.9-564.7 °C with the peak area under the DSC curve -4273,3 kJ/kg and with the maximum at 524.2 °C. Both the thermal processes are accompanied by significant weight losses.

On a DSC curve of the sample FB-9 two peaks were detected corresponding to exothermic processes. The first exothermic process occurs in the temperature interval 183.3-255.9 °C with the maximum at 230.2 °C and with the peak area under the DSC curve -1033,3 kJ/kg. The second exothermic process occurs in the temperature interval 423,2-546,8 °C with the peak area under the DSC curve -3640,7 kJ/kg and with the maximum at 488.2 °C. Both the thermal processes are accompanied by significant weight losses.

On a DSC curve of the sample FB-10 one peak was detected corresponding to an endothermic process and two peaks corresponding to exothermic processes. The endothermic process occurs in the temperature interval 13.6-178.1 °C with the peak area under the DSC curve 1953,1 kJ/kg, which is probably associated with a delay in heat transfer to the sample. The process reaches the minimum at 72.5 °C. The first exothermic process occurs in the temperature interval 192.3-254.6 °C with the maximum at 226.7 °C and with the peak area under the DSC curve at -865,5 kJ/kg. This process is accompanied by a significant weight loss. The second exothermic process occurs in the temperature interval 450.9-559.5 °C with the peak area under the DSC curve -3762.2 kJ/kg and with the maximum at 530.3 °C. Also this process is accompanied by a significant weight loss with a slight weight increase at the beginning.

The foils FB-6, FB-8, FB-9 and FB-10 prepared by joint oxidation of biochar with graphite are products with the same functional groups (see Tab. 4 and spectrums in Fig. 6 and 3c)). This is reflected by their very similar behavior during thermal analysis - see the TGA and DSC curves in Fig. 6, Fig. 4 and Fig. 3d. In all cases there are two exothermic processes with the maximums in the interval 212-230 °C. Slightly greater is the variation of temperatures of the second exothermal process where the maximums range from 488 to 530 °C. The lowest maximum temperature of degradation was found for the foil FB-9 which was made by oxidation with the lowest content of graphite. The total thermal changes of degradation of the foils FB-6, FB-8 and FB-9 are comparable but they are significantly lower than that of biochar FB-2 alone, which in this case was the initial component. Different types of biochar affected the resulting total thermal change of degradation of foils with the same ratio of graphite (1:2): FB-6 ($\sum$ H = - 4721 kJ/kg) in comparison with FB-10 ($\sum$ H = -6760 kJ/kg), which does not correspond to the values identified for thermal degradation of the initial biochars (sediment, flue ash). Biochar FB-2 was more exothermic (by 40 %) than FB-1 and the difference was 2294 kJ/kg. If we compare the total thermal change during degradation of foils prepared earlier (Klouda et al., 2014b) by oxidation of graphite alone and graphite with fullerene C60 (ratio 2:1) then we can see that the thermal change in case of the foil with biochar FB-2 (also the ratio 2:1) is higher and that the maximum temperature of the second exothermic effect is shifted to higher values, by up to 70-110 °C (depending on the graphite ratio).

Oxidation with H_2O_2, slight reduction with ascorbic acid and sonication resulted in thermal stabilization of biochar. We assume that "natural organic matter" adsorbed on the carbon skeleton of biochar was removed by chemical and physical reactions. We tested products of modified biochar in the temperature range 25-600 °C and the lowest weight loss was found for FB-3, i.e. for biochar

after sonication at a slightly elevated temperature. This product did not demonstrate any exothermic degradation. The thermal changes of degradation in case of the FB-4 (oxidation with H_2O_2) and FB-5 (reduction with ascorbic acid) were practically zero. The biggest weight loss in the measured temperature range was found for FB-7, i.e. a product of biochar oxidized using the Hummers method without presence of graphite.

Ignition temperature of biochar

Measuring of the minimum ignition temperature of biochar was performed in agreement with the standard ČSN EN 50281-2-1: Electrical apparatus for use in the presence of combustible dust - Part 2-1: Test methods - Methods for determining the minimum ignition temperatures of dust, method B: Swirling dust in an oven at a constant temperature. The measurement was performed on a modified instrument in which the method of dust swirling was modified: in the original instrument the dust is swirled into the test equipment from the top while in the modified instrument the dust is swirled from the bottom of the equipment. When using the swirling from the bottom the dust moves upwards and it is swirled. Subsequently, dust sedimentation occurs depending of the character of the dust, its properties and on the environment in which it is swirling. This method is supposed to keep the dust in the oven´s space longer and the sample exposure is therefore longer in comparison with the method anticipated by the standard.

The tested biochar sample was analyzed on sieves and the mean size of the particles was 0.13 mm.

The minimum ignition temperature of biochar is higher than 1000 °C. No explosion flame was observed on the biochar sample at the temperature of 1000 °C which is the ignition criterion for this test. Only sparks were observed during the measurement, which are not considered an ignition.

Interpretation and allocation of vibrations to IR spectrums

The basic difference between the measured spectrums of initial biochar was in the values of absorbance of the whole spectrum - see Fig. 2. The dominant peak in the FB-1 spectrum is a broad solid absorption band with the maximum at 3312 cm^{-1} allocated to the valence vibration of -OH. Weak valence vibrations for this group are also in the spectrum FB-2 with a shift of wave numbers to higher values. The principal difference between the spectrums is in the identification of weak but characteristic vibrations of the group -C=O in the biochar from the flue dust (FB-2) and its strongest vibration at 1405 cm^{-1}, which we allocated to the valence vibration of the -COO- anion. In the spectrums of both biochars there are vibrations that can be potentially allocated to an aromatic skeleton and related summation bands of aromatic rings (2000-2300 cm^{-1}) and there are central valence vibrations of the groups C-O, C-O-C, =C-O (FB-1 1034 cm^{-1}, FB-2 1031 cm^{-1}).

Two oxidations of biochar have been also described in literature with aggressive oxidizing (nitrating) agents. The initial biochar was prepared at 350 °C from rice straw and hulls and its oxidation was performed with a mixture of HNO_3/H_2SO_4 (1:3) that was diluted for experimental purposes to 20, 40 and 60 % (Liu et al., 2015). This oxidation resulted in a product with good adsorption ability to Cd and Al ions. In the second case (Qian et al., 2015) the oxidation was performed with 50 % nitric acid at 60 °C and the reaction time was 5 hours. Equally as in our work, FT-IR analysis was used for basic identification of functional groups. The published IR spectrum (Liu et al., 2015) has the strongest absorbance at 1106 cm^{-1} C-O-C, 3420 cm^{-1} -OH, 1720 cm^{-1} C=O. The peak at 1610 and 1444 cm^{-1} was allocated to the asymmetric and symmetric vibrations -COO-. At the same time, a very weak peak at 1346 cm^{-1} was assigned to the symmetric vibration $-NO_2$ and the authors assumed electrophilic substitution of hydrogen on the carbon skeleton. A medium strong vibration with the maximum at 3420 cm^{-1} was assigned to the bond vibration -OH. In case of the second experiment (Qian et al., 2015) the authors believed that a part of biochar formed nanoparticles soluble in water. This solubility was possible due to the presence of the groups -COOH (1717 cm^{-1}) and -OH. For our product (FB-7), i.e. product of oxidation of biochar without graphite using the Hummers method, we were not able to identify any vibrations characteristic for -OH groups. Weak vibrations in the spectrum at 2671 cm^{-1} and 2604 cm^{-1} can be assigned to C-H. Medium vibrations 1719 cm^{-1} and 1702 cm^{-1} have been assigned to carbonyl and vibrations at 1560 cm^{-1} to aromatic skeleton (C=C), and they continue with summation bands of the aromatic ring (2000-2300 cm^{-1}). The absorbance had the maximum at 1074 cm^{-1} and it can be assigned to functional groups C-O, asymmetric and symmetric C-O-C, =C-O-C or to their structural groupings. In our IR spectrum we have not identified any vibration of the $-NO^2$ group (Liu et al., 2015) 1540 cm^{-1} and 1348 cm^{-1}/.

We were surprised by the absence of -OH groups in the product of oxidation. However, their absence was apparent even earlier, when the product was processed by decantation and centrifugation and when we were unable to produce a thick oily suspension - interconnection by hydrogen bonds that enable formation of a foil (film). The water suspension looked like a "colloid", homogeneously dispersed, and most of it passed through a filter. A broad and intense absorption band characterizing the -OH vibration was identified in foils made of the products FB-6 and FB-10 after oxidation of biochars in presence of graphite (2:1) and regardless of the initial type of biochar - see Fig. 3. Spectrums of the foils were very similar, with certain differences e.g. in intensity of absorbances of the groups C=O and C=C, -C= C-C=C-, which was more intense in the foil FB-6. Naturally, there are also small differences in the wave numbers and shapes of the peaks in the interval 1020-1300 cm^{-1} which is characteristic for valence vibrations of C-O-C, = C-O-C, -O- (ether, ester, anhydride, acetal). Presence of graphite in biochar oxidation influenced properties of the prepared products. IR spectrums (Fig. 6) were used to identify joint functional groups and their allocation to wave numbers - see Table IV. There was a certain small difference between the products FB-6, FB-8 and FB-9 in the shift of the strong vibration which characterizes oxy groups, specifically towards the higher values with a decrease of graphite content in the oxidized mixture (Fig. 7, 8).

The method selected for pilot testing to determine phytotoxicity of biochar and its modifications was a contact test of inhibition of germinability and root growth. The selected test organism was white mustard (*Sinapis alba L.*). The tests were performed based on a modified procedure described in Annex No. 1 to the Methodic instruction by the waste department for determination of ecotoxicity of wastes (G. Fang et al., 2014). For a control sample 20 seeds were evenly distributed on wet filtration paper placed on a Petri dish. For the tested samples, with regard to the limited quantity of the prepared nanomaterials, a specific sample weight was placed into each dish - see Tab. 2 (2 parallel determinations for each sample). 10 seeds were placed on the weighted sample and 10 more seeds were evenly distributed around the sample, similarly as in the control sample. The seeds were incubated in the dark at 21 °C for 72 hours.

As indicated by Tab. 2 the root growth was least affected by the sample FB4. The other samples slowed down the root growth much more and their inhibition effects were essentially comparable, while the most toxic ones seemed to be the samples FB6 and FB8. No significant inhibition effects were observed for the seeds placed outside the samples, with one exception of the sample FB10. Even some positive effects on the root growth were observed in the proximity of the samples and the effect was again most distinct for the sample FB4 (see Fig. 5). However, we used only a limited number of seeds for the pilot testing and therefore the results are rather informative.

Summary results of toxicity of biochar and its modification

Tab. 2 Average values of seed germination ability and root growth inhibition (IC)

Material	Average sample weight [g]	Average germination ability of seeds outside/on the foil	Average IC of seeds on the sample	Average IC outside the samples
FB 1	-*	-*	-*	-*
FB 2	-**	-**	-**	-**
FB 3	0.3856	100/100	50.09	-33.33
FB 4	0.1950	100/100	-26.14	-104.55
FB 5	0.2617	100/100	46.02	-31.82
FB 6	0.03598	35/100	93.60	-2.90
FB 7	-***	-***	-***	-***
FB 8	0.0220	50/95	85.75	-1.16
FB 9	0.0179	90/95	61.47	8.52
FB 10	0.0087	100/100	61.86	24.60

Legen:
* it was not possible to evaluate the test,
** the value was determined at IC50 54.65 ± 1.15 g/l,
*** it was not possible to perform the test for the sample.

Conclusions

Biochar is a product obtained from processing of waste biomass. Oxidation of biochar in presence of graphite enables preparation of foils with a lamellar structure (Klouda et al., 2014b) with modifications that provides them with a potential for future applications. In this article there are further described the results of thermal stability of prepared products also ignition temperature of biochar was measured. Finally there were discussed interpretation and allocation of vibrations to IR spectrums and the toxicity of various types of biochar.

Acknowledgements

The authors express their thanks to Ing. Eva Zemanová, Ph.D. for quality service provided during measurement of IR spectrums, to Mgr. Eliška Brabencová for her help with synthesis, to Ing. Petr Lepík, Ph.D. for his help with the ignition temperature test and, last but not least, to Mgr J. Senčík for technical support. This contribution was prepared within the Student Grant Competition SP2016/92 "Evaluation of environmental effects of selected nanomaterials and products of thermal degradation of materials after their contact with water from the viewpoint of ecotoxicity".

References

Abdul Hamid, S.B., Chovdury, Z.Z., Zain, S.M. 2014. Base catalytic approach: A promising technique for the activation of biochar for equilibrium sorption studies of Copper, Cu(II) ions in single solute system. Materials (Basel), 7(4): 2815-2832. doi:10.3390/ma7042815.

Ahmad, M., Lee, S.S., Rajapaksha, A.U., Vithanage, M., Zhang, M., Cho, J.S., Lee, S.E., Ok, Y.S. 2013. Trichloroethylene adsorption by pine needle biochars produced at various pyrolysis temperatures. Bioresour. Technol., 143: 615-622. doi:10.1016/j.biortech.2013.06.033.

Das, O., Sarmah, A.K., Bhattacharryyat, D. 2015. A sustainable and resilient approach through biochar addition in wood polymer composites. Sci. Total Environ., 512-513: 326-336. doi:10.1016/j.scitotenv.2015.01.063.

Dzonzi-Undi, J., Masek, O., Abass, O. 2014. Determination of Spontaneous Ignition Behaviour of Biochar Accumulations. Int. J. Sci. Res., 3(8): 656-661.

Essandoh, M.n, Kunwar, B., Pittman, C.U., Mohan, D., Mlsna, T. 2015. Sorptive removal of salicylic acid and ibuprofen from aqueous solutions using pine wood fast pyrolysis biochar. Chem. Eng. J., 265: 219-227. doi:10.1016/j.cej.2014.12.006.

Fang, C., Zhang, T., LI, P., Jiang, R.F., Wang, Y.C. 2014. Application of magnesium modified corn biochar for phosphorus removal and recovery from swine wastewater. Int. J. Environ. Res. Public Health, 11(9): 9217-9237. doi:10.3390/ijerph110909217.

Fang, G., Gao, J., Liu, C., Dionysiou, D.D., Wang, Y., Zhou, D. 2014. Key role of persistent free radicals in hydrogen peroxide activation by biochar: Implications to organic contaminant degradation. Environ. Sci. Technol., 48(3): 1902-1910. doi:10.1021/es4048126.

Gu, Z., Wang, X. 2013. Carbon Materials from High Ash Biochar: A Nanostructure Similar to Activated Graphene. Am. Trans. Eng. Appl. Sci., 2: 15-34.

Chen, B., Chen, Z. 2009. Sorption of naphthalene and 1-naphthol by biochars of orange peels with different pyrolytic temperatures. Chemosphere, 76(1): 127-133. doi:10.1016/j.chemosphere.2009.02.004.

Chen, X., Chen, G., Chen, L., Chen, Y., Lehmann, J., Mcbride, M.B., Hay, A.G. 2011. Adsorption of copper and zinc by biochars produced from pyrolysis of hardwood and corn straw in aqueous solution. Bioresour. Technol., 102(19): 8877-8884. doi:10.1016/j.biortech.2011.06.078.

IM, J.K., Boateng, L.K., Flora, J.R. V, Her, N., Zoh, K.D., Son, A., Yoon, Y. 2014. Enhanced ultrasonic degradation of acetaminophen and naproxen in the presence of powdered activated carbon and biochar adsorbents. Sep. Purif. Technol., 123(26): 96-105. doi:10.1016/j.seppur.2013.12.021.

Inyan, M., Gao, B., Zimmerman, A., Zhang, M., Cem, H. 2014. Synthesis, characterization, and dye sorption ability of carbon nanotube-biochar nanocomposites. Chem. Eng. J., 236 (15), p. 39-46. doi:10.1016/j.cej.2013.09.074.

Jing, X.-R., Wang, Y.-Y., Liu, W.-J., Wang, Y.-K., Jiang, H. 2014. Enhanced adsorption performance of tetracycline in aqueous solutions by methanol-modified biochar. Chem. Eng. J., 248(15): 168-174. doi:10.1016/j.cej.2014.03.006.

Jung, K.W., Hwang, M.J., Jeong, T.U., Ahn, K.H. 2015. A novel approach for preparation of modified-biochar derived from marine macroalgae: Dual purpose electro-modification for improvement of surface area and metal impregnation. Bioresour. Technol., 191: 342-345. doi:10.1016/j.biortech.2015.05.052.

Karim, A., Manish, K., Sangamitra, M., Sing. 2015. Banana Peduncle Biochar: Characteristics and Adsorption of Hexavalent Chromium from Aqueous Solution. Int. Res. J. Pure Appl. Chem., 7(1). doi:10.9734/IRJPAC/2015/16163.

Klouda, K., Friedrichova, R., Lach, K., Zemanova, E. 2014a. Thermal Stability of Graphene Oxide and its Derivatives Selected, In Šenovský, M. (Ed.): Fire Protection 2014. SPBI, Ostrava. (in Czech)

Klouda, K., Zemanova E., Brabencova, E., Bradka, S., Dvorsky, R. 2014b. Joint Oxidation of Fullerene C 60 and Graphite. Int. J. Emerg. Technol. Adv. Eng., 4(10): 504-522.

Krishnakumar, S., Rajalaskhmi, A.G., Balaganesh, B., Manikadan, P., Vinoth, C., Rajendran, V. 2014. Impact of Biochar on Soil Physical Properties. Int. J. Adv. Res., 2(4): 933-950.

Kumar, S., Loganathan, V.A., Gupta, R.B., Barnett, M.O. 2011. An Assessment of U(VI) removal from groundwater using biochar produced from hydrothermal carbonization. J. Environ. Manage., 92 (10): 2504-2512. doi:10.1016/j.jenvman.2011.05.013.

Lehmann, J., Rilling, M., Thies, J., Masilleo, C. A, Hockday, W.C., Crowley, D. 2011. Biochar effects on soil biota-A review. Soil Biol. Biochem., 43(9): 1812-1836. doi:10.1016/j.soilbio.2011.04.022.

Li, Y., Shao, J., Wang, X., Deng, Y., Yang, H., Chen, H. 2014. Characterization of modified biochars derived from bamboo pyrolysis and their utilization for target component (furfural) adsorption. Energy and Fuels, 28 (8): 5119-5127. doi:10.1021/ef500725c.

Liao, P., Zhan, Z., Dai, J., Wu, X., Zhang, W., Wang, K., Yuan, S. 2013. Adsorption of tetracycline and chloramphenicol in aqueous solutions by bamboo charcoal: A batch and fixed-bed column study. Chem. Eng. J., 228: 496-505. doi:10.1016/j.cej.2013.04.118.

Liu, P., Liu, W.J., Jiang, H., Chen, J.J., Li, W.W., Yu, H.Q. 2012. Modification of bio-char derived from fast pyrolysis of biomass and its application in removal of tetracycline from aqueous solution. Bioresour. Technol., 121: 235-240. doi:10.1016/j.biortech.2012.06.085.

Liu, W.J., Jiang, H., Yu, H.Q. 2015. Development of Biochar-Based Functional Materials: Toward a Sustainable Platform Carbon Material. Chem. Rev. doi:10.1021/acs.chemrev.5b00195.

Liu, Z., Quek, A., Kent Hoekman, S., Srinivasan, M.P., Balasubramanian, R. 2012. Thermogravimetric investigation of hydrochar-lignite co-combustion. Bioresour. Technol., 123: 646-652. doi:10.1016/j.biortech.2012.06.063.

Lu, H., Zhang, W., Yang, Y., Huang, X., Wang, S., Qiu, R. 2012. Relative distribution of Pb2+ sorption mechanisms by sludge-derived biochar. Water Res., 46 (3): 854-862. doi:10.1016/j.watres.2011.11.058.

Manav, S., Sheli, M., Sabyasachi, S. 2016. Carbon nanoparticles in “biochar” boost wheat (Triticum aestivum) plant growth, RSC Adv. doi:10.1039/C4RA06535B.

Oh, S.Y., Seo, Y.D. 2015. Factors Affecting Sorption of Nitro Explosives to Biochar: Pyrolysis Temperature, Surface Treatment, Competition, and Dissolved Metals. J. Environ. Qual., 44 (3):833. doi:10.2134/jeq2014.12.0525.

Oh, S.Y., Seo, Y.D. 2014. Sorptive Removal of Nitro Explosives and Metals Using Biochar. J. Environ. Qual., 43(5):1663. doi:10.2134/jeq2014.02.0097.

Oleszczuk, P., Hale, S.E., Lehnmann, J., Cornelissen, G. 2012. Activated carbon and biochar amendments decrease pore-water concentrations of polycyclic aromatic hydrocarbons (PAHs) in sewage sludge. Bioresour. Technol., 111: 84-91. doi:10.1016/j.biortech.2012.02.030.

Qian, L., Chen, M., Chen, B. 2015. Competitive adsorption of cadmium and aluminum onto fresh and oxidized biochars during aging processes. J. Soils Sediments, 15(5): 1130-1138. doi:10.1007/s11368-015-1073-y.

Safarik, I., Horska, K., Pospiskova, K., Safarikova, M. 2012. Magnetically responsive activated carbons for bio-and environmental applications. Int. Rev. Chem. Eng., 4 (3): 346-352.

Shan, D., Deng, S., Zhao, T., Wang, B., Wang, Y., Huang, J., Yu, G., Winglee, J., Wiesnerr, M.R. 2016. Preparation of ultrafine magnetic biochar and activated carbon for pharmaceutical adsorption and subsequent degradation by ball milling. J. Hazard. Mater., 305: 156-163. doi:10.1016/j.jhazmat.2015.11.047.

Shen, Y. 2015. Chars as carbonaceous adsorbents/catalysts for tar elimination during biomass pyrolysis or gasification. Renew. Sustain. Energy Rev., 43: 281-295. doi:10.1016/j.rser.2014.11.061.

Schmidt, H.P., Wilson, K. 2014. The 55 uses of biochar [WWW Document]. Biochar J. URL https://www.biochar-journal.org/en/ct/2 (accessed 1.11.17).

Sun, K., Keiluweit, M., Kleber, M., Pan, Z., Xing, B. 2011. Sorption of fluorinated herbicides to plant biomass-derived biochars as a function of molecular structure. Bioresour. Technol., 102(21): 9897-9903. doi:10.1016/j.biortech.2011.08.036.

Taha, S.M., Amer, M.E., Elmasafry, A.E., Elkady, M.Y. 2014. Adsorption of 15 different pesticides on untreated and phosphoric acid treated biochar and charcoal from water. J. Environ. Chem., Eng. 2 (4): 2013-2025. doi:10.1016/j.jece.2014.09.001.

Tan, X. F., Liu, Y. G., Gu, Y. L., Xu, Y., Zeng, G. M., Hu, X. J., Liu, S. B, Wang, X., Liu, S. M., Li, J. 2016. Biochar-based nano-composites for the decontamination of wastewater: A review. Bioresour. Technol., 212:318-333. doi:10.1016/j.biortech.2016.04.093.

Tan, X., Liu, Y., Zeng, G., Wang, X., Hu, X., Gu, Y., Yang, Z.: 2015. Application of biochar for the removal of pollutants from aqueous solutions. Chemosphere., 125: 70-85. doi:10.1016/j.chemosphere.2014.12.058.

Tang, J., Li, X. Luo, Y., Li, G., Khan, S. 2016. Spectroscopic characterization of dissolved organic matter derived from different biochars and their polycylic aromatic hydrocarbons (PAHs) binding affinity. Chemosphere., 152: 399-406. doi:10.1016/j.chemosphere.2016.03.016.

Trigo, C., Spokas, K.A., Cox, L., Koskinen, W.C. 2014. Influence of soil biochar aging on sorption of the herbicides MCPA, nicosulfuron, terbuthylazine, indaziflam, and fluoroethyldiaminotriazine. J. Agric. Food Chem., 62 (45): 10855-10860. doi:10.1021/jf5034398.

Wang, S., Gao, B., Li, Y., Mosa, A., Zimmerman, A.R., Ma, L.Q., Harris, W.G., Migliaccio, K.W. 2015. Manganese oxide-modified biochars: Preparation, characterization, and sorption of arsenate and lead. Bioresour. Technol., 181: 13-17. doi:10.1016/j.biortech.2015.01.044.

Wang, Y., Wang, L., Fang, G., Herath, H.M.S.K., Wang, Y., Cang, L., Xie, Z., Zhou, D. 2013. Enhanced PCBs sorption on biochars as affected by environmental factors: Humic acid and metal cations. Environ. Pollut., 172: 86-93. doi:10.1016/j.envpol.2012.08.007.

Yakou, S.M., El, A., Daifullah, H.M., El-reefy, S.A. 2015. Pore structure characterization of chemically modified biochar derived from rice straw. Environmental, 14 (2): 473-480.

Yang, G.X., Jiang, H. 2014. Amino modification of biochar for enhanced adsorption of copper ions from synthetic wastewater. Water Res., 48: 396-405. doi:10.1016/j.watres.2013.09.050.

Yao, Y., Gao, B., Fang, J., Zhang, M., Chen, H., Zhou, Y., Elise, A., Sun, Y., Yang, L. 2014. Characterization and environmental applications of clay - biochar composites. Chem. Eng. J., 242: 136-143.

Yao, Y., Wu, F. 2015. Naturally derived nanostructured materials from biomass for rechargeable lithium/sodium batteries. Nano Energy., 17: 91-103. doi:10.1016/j.nanoen.2015.08.004.

Zhang, L., Jiang, J., Holm, N., Chen, F. 2014. Mini-chunk biochar supercapacitors. J. Appl. Electrochem., 44(10): 1145-1151. doi:10.1007/s10800-014-0726-7.

Zhang, M., Gao, B., Yao, Y., Xue, Y., Inyang, M. 2012. Synthesis, characterization, and environmental implications of graphene-coated biochar, Science of The Total Environment., 435-436:567-572.doi:10.1016/j.scitotenv.2012.07.038.

Zhou, Y., Gao, B., Zimmerman, A.R., Fang, J., Sun, Y., Cao, X. 2013. Sorption of heavy metals on chitosan-modified biochars and its biological effects. Chem. Eng. J., 231: 512-518. doi:10.1016/j.cej.2013.07.036.